Chalcogenide Letters Vol. 6, No. 9, September 2009, p. 517 – 522

NANO AND MICROSTRUCTURES OF SELENIUM OXIDE BY THERMAL EVAPORATION

Karunapati Tripathi, M. Husain, M. Zulfequar*
Department of Physics, Jamia Millia Islamia, New Delhi.

In the present work synthesis of selenium oxide nano and microstructures at particular oxygen pressure and different substrate temperature is reported. Pure selenium powder is evaporated via thermal evaporation at different substrate temperature, i.e. at liquid nitrogen temperature and room temperature in presence of oxygen. The chamber pressure was kept at 4 Torr for different substrate temperature. The UV-visible spectra show the optical band gap of 2.8 eV & 3.53 eV for samples deposited at room temperature and liquid nitrogen temperature. Surface morphology and elemental analysis was done using Scanning Electron Microscopy (SEM) & x-ray diffraction (XRD) technique. SEM pictures show the spherical balls of selenium oxide having size of the order of 300-500 nm & 40-100 nm. .

(Received August 26, 2009; accepted September 29, 2009)

Keywords: Nanostructures, Optical band gap, SEM, XRD.

1. Introduction

There has been much interest in one-dimensional nanoscale or submicron scale due to their potential in mesoscopic and nanodevice technique. As important member of semiconductor family, Se & Te show unique physical and chemical properties which provide them with the chances to widen the range of applications [1-6]. Semiconductor nano-particles have attracted much attention over the past few years because of their novel electrical and optical properties; originated from quantum confinement of charge carriers [7-10].

With the discovery of oxide nanobelts of semiconducting oxides in 2001 [11], research into functional based, one dimensional nanostructures has rapidly extended because of their unique and novel applications in optics, optoelectronics, catalysis and piezoelectricity.

Exemplary oxide nanostructures that can be fabricated according to the inventive processes include semiconducting or dielectric oxides such as ZnO, TiO_2 , MnO_2 , SnO, ZrO_2 , V_2O_5 , SiO_2 , CrO_2 , Cr_2O_3 , MgO, Al_2O_3 ferroelectric oxides (such as $BaTiO_3$, $(Pb,La)(Zr,Ti)O_3$, $SrBi_2Ta_2O_9$, and $(Bi,La)_4Ti_3O_{12}$), magnetic oxides (such as magnetite, Ba-ferrite, Ni—Zn ferrite), superconductive oxides (such as $YBa_2Cu_3O_7$), and magneto-resistive oxides (such as La—Ca—Mn—O or La—Sr—Mn—O).

With other semiconductor oxides, selenium is naturally found in number of crystalline structure; trigonal (helical chain), monoclinic (Se8 rings) as well as amorphous structures e.g. mixture of disorder chain. It is photo conducting material with high refractive index and high reactivity with low melting point of ~ 217^o C. In the present work we report synthesis of selenium oxide nano and microstructures via thermal condensation/evaporation at different temperatures. The idea of growth of this oxide is inspired by the growth of nanostructures of semi conducting oxide in 2001. [12].

The morphology of nanostructures is decided depending on the application. Therefore it is of quite great interest to synthesize selenium oxide nanostructures which may be used for

* Corresponding author: mzulfe@rediffmail.com

optoelectronic application. As grown samples were characterized using Scanning Electron Microscope (SEM), UV-visible absorption spectroscopy (UV-vis) and X-ray diffraction analysis (XRD).

2. Experimental

Selenium oxide micro/nanostructures are grown on the glass substrate by thermal condensation/evaporation technique at 4 Torr in oxygen ambient. The pure selenium powder is placed in molybdenum (Mo) boat as source material. Base pressure of chamber is achieved to 10^{-6} Torr and then oxygen gas is passed to maintain chamber pressure 4 Torr through the evaporation process. Selenium is then evaporated by resistive heating of Mo boat. It is expected to react selenium with available oxygen present in the chamber before deposition on substrate which are kept at two different temperatures once at room temperature and again for liquid nitrogen temperature i.e. 77 K. Figure 1 shows the schematic of specially designed chamber. It consists of electrodes for resistive heating of Mo boat, way to insert gas using needle valve, pressure gauge to monitor the required pressure in chamber and substrate holder which can be cooled to liquid nitrogen temperature as exhibited in the diagram. Surface morphology of the as grown samples are studied under SEM (JEOL 6380), UV-Vis absorption spectra were obtained using Camspec spectrophotometer (M 550) for calculation of band gap. XRD studies are carried out using X-ray diffractometer (Philips PW 1830/40) using Cu Kα radiations (λ=1.5412 A^o).

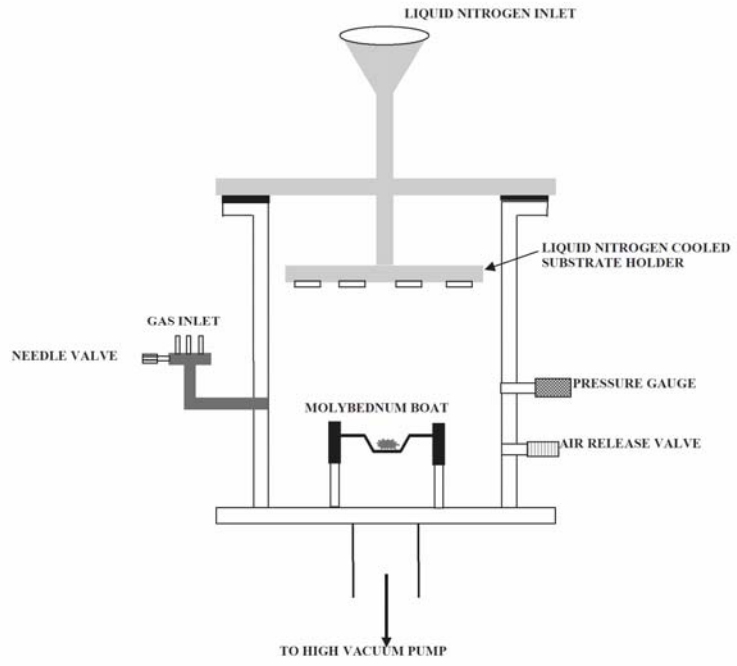

Fig. 1. Schematic of vacuum chamber.

3. Results and discussion

Fig. 2 (a) & (b) shows SEM images of selenium oxide deposited at different substrate temperature at 4 Torr oxygen pressure. Fig 2(a) & (b) are the SEM images of as grown thin films at RT and LN_2 temperatures.

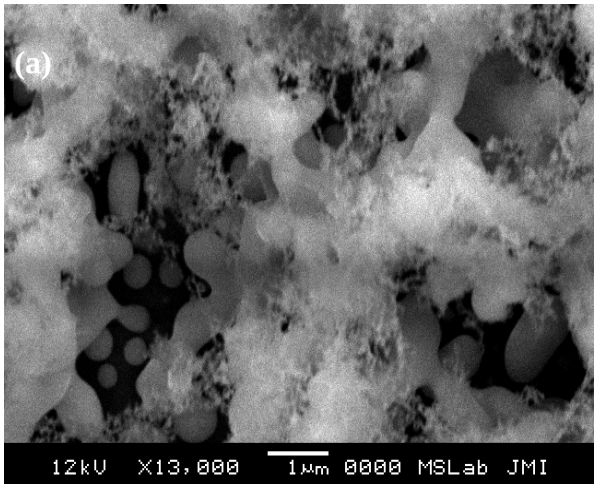

Fig. 2(a) SEM micrograph of room temperature grown selenium oxide structure.

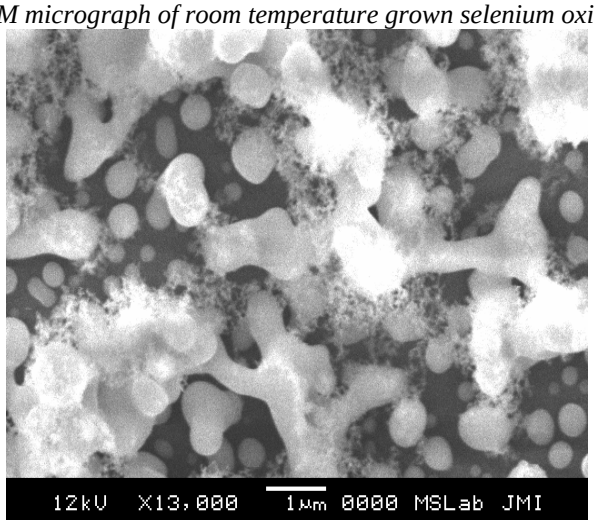

Fig. 2(b) SEM micrograph of LN_2 temperature grown selenium oxide structure.

The interesting spherical ball like structures of different size is grown on glass substrate both at RT & as well as LN_2 temperature. At room temperature some stretched spring like structures are also observed mixed with spherical balls on glass surface where as at LN_2 temperature spring like structures disappear and uniform and stable spherical balls are observed. This is due to surface energy minimization at LN_2 temperature. The particle size obtained at RT growth is of the order of ~ 300-500 nm and that of LN_2 is found between 50-100 nm with some of the ball coalescence forming the bigger structures (in µm order) on the surface. This suggests that uniform ball like structures of selenium oxide can be grown under controlled condition. In case of room temperature formation of polymer chain like structures are evidence of selenium/selenium oxide.

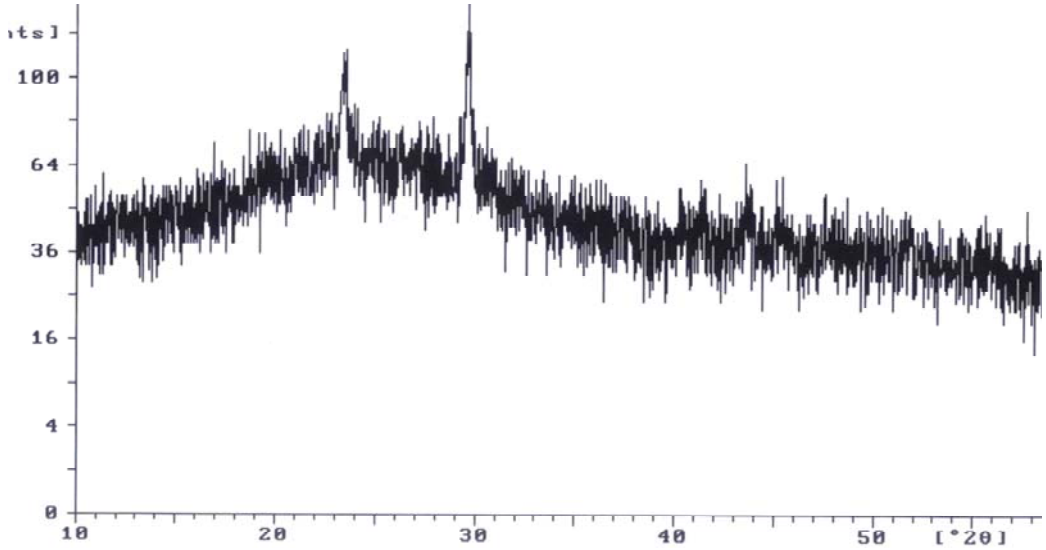

Fig. 3(a) XRD pattern of as grown thin film of selenium oxide at room temperature.

Fig. 3(a & b) is the typical XRD pattern of the samples as grown at different substrate temperature(at RT and at LN_2 temperature). XRD pattern of room temperature grown sample show two peaks of Se_2O_5 of different orientations (110) & (014) as matched to standard JCPDS data [13]. In case of the sample grown at liquid nitrogen temperature, the intensity of the peaks are low which suggest the small particle size of Se_2O_5 nanostructures. The Sherrer equation is used to calculate the size of these structures. The equation is as

$$crystallite'size = \frac{0.9 \times \lambda}{\cos\beta \times FWHM} \tag{1}$$

where λ is the wavelength of X-ray used, it is 1.54 A^o in our case. β is the angle of the peak position. FWHM is the full width at half maxima. The size of the Se_2O_5 nanosprings is found to be 50nm and 40 nm. XRD spectra shows some other orientations of the grown structures including (110), (014), (120), (032) and (130).

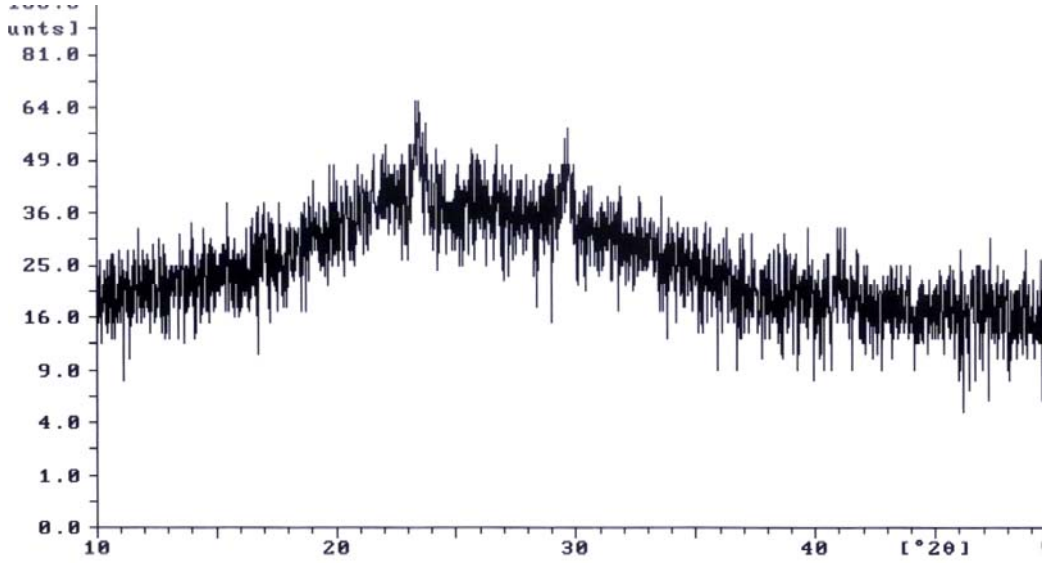

Fig. 3(b) XRD pattern of as grown thin film of selenium oxide at LN_2 temperature.

The band gap of selenium oxide is estimated from the absorption spectra of each grown thin film obtained in the wavelength range of 200 nm to 1100 nm. The absorption coefficient (α) is calculated from the spectra using the following relation

$$\alpha = \frac{OD}{t} \tag{2}$$

where OD is the optical density values obtained from spectrometer data, 't' is the thickness of the film which was kept constant of 300 nm.

The value of the extinction coefficient (k) is calculated from following relation,

$$k = \frac{\alpha\lambda}{4\pi} \tag{3}$$

where α is absorption coefficient at particular wavelength λ.

The value of the direct band gap for all the grown nanostructures were obtained using Tauc plot of $(\alpha h\nu)^{1/2}$ vs energy (hν) shown in fig 4.

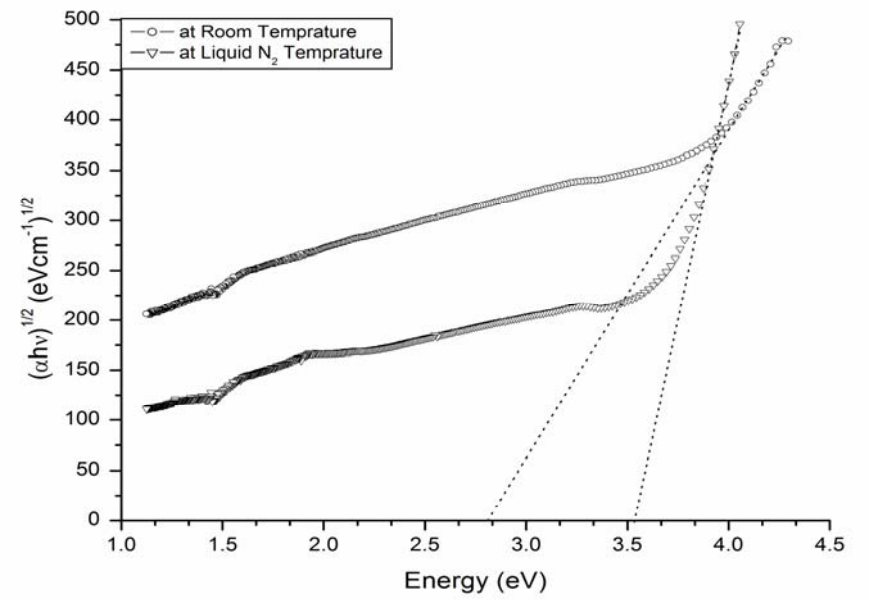

Fig. 4. Tauc plot for the absorption spectra of grown films at RT and LN_2 temperature.

The tangent drown at absorption edge was extrapolated to energy axis i.e. zero absorption and the intercept gives value of the band gap. The optical band gap obtained from Tauc plot (Fig 4.) value is 2.81 eV and 3.53 eV for the films deposited at room temperature and LN_2 temperature respectively where as the typical value of optical band gap of the pure selenium thin amorphous film is 2.05 eV [14]. There is increase in the value of the band gap at LN_2 temperature grown sample which may be attributed to confinement of the size of the selenium oxide as observed from the SEM pictures. Optical properties of the nanostructure systems are influenced by the confinement effect, producing a blue shift in the optical spectra. The quantum confinement effect shifts the band gap of a bulk semiconductor to higher energy. This shift is called the confinement energy, depends on the size and shape of the material. Table 1 shows the calculated values of the parameters of the grown samples.

Table 1. Various parameters calculated for as grown samples of Selenium Oxide

	α (cm^{-1}) (at 500 nm)	E_g (eV)	(h k l)	k (at 500 nm)	Structure size (nm)
Room Temperature	36.08	2.8	(110) & (014)	.1436	300-500
Liquid Nitrogen Temperature	13.13	3.53	(110), (014), (120), (032) & (130).	.0104	40-100

4. Conclusion

We have grown nanostructures of selenium oxide of the form Se_2O_5 at RT and at LN_2 temperature with different orientations. The XRD pattern suggests the low particle size of the grown films grown at LN_2 temperature. SEM micrograph shows the particles size in nm range and stretched spring like structures mixed with spherical balls at room temperature. Optical absorption study implies that films grown at RT has lower value of band gap and, whereas films grown at LN_2 temperature exhibit higher value of these parameters. The substrate temperature have major role in the size determination as we have deposited microstructures of Se_2O_5 (300-500nm) at 300K (RT), whereas at LN_2 (77K) temperature the size of the structures reduced to nanostructures (40-100 nm). This shows that the band gap can be engineered by varying the deposition conditions.

References

[1] P. Tangney, S. Fahy, Phys. Rev B **65**, 054302 (2002).
[2] X. Duan, Y. Huang, Y. Cui, J. Wang and C.M. Lieber, Nature **409**, 66 (2001).
[3] H.M.Huang, S. Mao, H. Feick, H. Yan, Y. Wu, H. Kind, E. Weber, R. Russo and P. Yang, Science **292,** 1897 (2001).
[4] S. W. Chung, J.Y. Yu, J. R. Heath, Appl. Phys. Lett. **76**, 2068 (2000).
[5] D. T. Schoen, C. Xie and Y.Cui, J. Am. Chem. Soc. **129**, 4116 (2007).
[6] H. H. Yang, S.Q. Zhang, F. Tan, Z.X. Zhuang and X.R. Wang, J. Am. Chem. Soc. **127**, 1378 (2005).
[7] Y Wang and N Herron, J. Phys. Chem. **95**, 525 (1991).
[8] P.V. Kamat J. Phys. Chem. B **106**, 7729 (2002).
[9] B. Zhang, X. Ye, W Dai, W Hou, F. Zuo and Y Xie, Nanotechnology **17**, 385 (2006).
[10] I. Chakraborty and S.P. Moulik, J. Nanopart. Res. **6**, 233 (2004).
[11] Z.W. Pan, Zu Rong Dai and Z.L. Wang, Science **291**, 1947 (2001).
[12] Pan Z. W. Dai Z. R. and Wang Z. L. Science, **291**, 1947 (2001).
[13] Z. Zak, Dostal Collect Czech Commun. **43**, 2509 (1978).
[14] J. P. Audiere, C. Mazieres, J. C. Carballes, J. Non-Cryst Solids **27**, 411 (1978).